Volume 14
Number 35
21 September 2023
Pages 9231–9614

Chemical Science

rsc.li/chemical-science

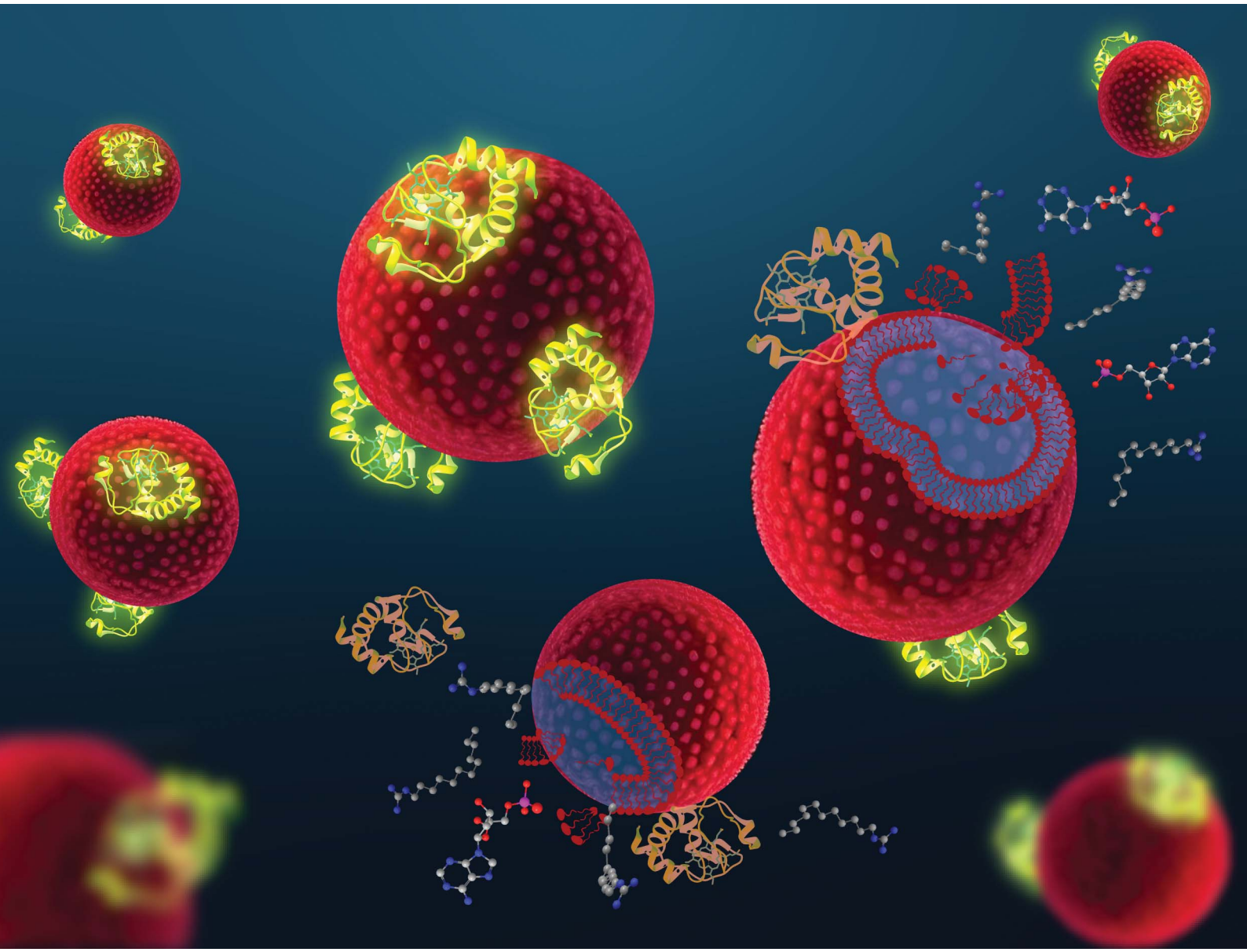

ISSN 2041-6539

ROYAL SOCIETY OF CHEMISTRY

EDGE ARTICLE

Subinoy Rana *et al.*

A transient vesicular glue for amplification and temporal regulation of biocatalytic reaction networks

Chemical Science

ROYAL SOCIETY OF CHEMISTRY

EDGE ARTICLE

View Article Online
View Journal | View Issue

Cite this: *Chem. Sci.*, 2023, **14**, 9267

All publication charges for this article have been paid for by the Royal Society of Chemistry

A transient vesicular glue for amplification and temporal regulation of biocatalytic reaction networks†

Alisha Kamra, Sourav Das, Preeti Bhatt, Manju Solra, Tanmoy Maity and Subinoy Rana *

Regulation of enzyme activity and biocatalytic cascades on compartmentalized cellular components is key to the adaptation of cellular processes such as signal transduction and metabolism in response to varying external conditions. Synthetic molecular glues have enabled enzyme inhibition and regulation of protein–protein interactions. So far, all the molecular glue systems based on covalent interactions operated under steady-state conditions. To emulate dynamic biological processes under dissipative conditions, we introduce herein a transient supramolecular glue with a controllable lifetime. The transient system uses multivalent supramolecular interactions between guanidinium group-bearing surfactants and adenosine triphosphate (ATP), resulting in bilayer vesicle structures. Unlike the conventional chemical agents for dissipative assemblies, ATP here plays the dual role of providing a structural component for the assembly as well as presenting active functional groups to "glue" enzymes on the surface. While gluing of the enzymes on the vesicles achieves augmented catalysis, oscillation of ATP concentration allows temporal control of the catalytic activities similar to the dissipative cellular nanoreactors. We further demonstrate temporal upregulation and control of complex biocatalytic reaction networks on the vesicles. Altogether, the temporal activation of biocatalytic cascades on the dissipative vesicular glue presents an adaptable and dynamic system emulating heterogeneous cellular processes, opening up avenues for effective protocell construction and therapeutic interventions.

Received 12th January 2023
Accepted 27th July 2023

DOI: 10.1039/d3sc00195d

rsc.li/chemical-science

Introduction

Temporal control of biomolecular components is key to several intracellular reaction networks,[1] robust signal transductions,[2] and efficient cell–cell communications.[3] Likewise, temporal regulation of enzyme activities allows dynamic control of biological transduction[4] and metabolism amongst other processes, helping elucidate biological events at the molecular level[5] and develop therapeutics with low side effects.[6] While compartmentalized vesicles[7] or scaffold protein-mediated assembly of enzymes[8] allow organization of functional components inside the cell, dynamic regulation of activities requires transient assemblies in response to the stimuli.[9] Non-covalent interactions enable transient assembly of the active components inside the cell to introduce the dynamic regulatory behavior affecting biomolecular reaction networks,[10,11] assembly of cytoskeletal filaments,[12] cross-talk with organelles,[13,14] and receptor clustering on lipid membranes.[15,16] Further, multiple weak non-covalent interactions such as electrostatics, hydrogen-bonding and van der Waals forces cause adhesion aiding in various biological processes such as the recruitment of white blood cells to inflamed tissue,[17] adherence of influenza virus,[18] and cell division.[19] Synthetic supramolecular systems featuring multivalent non-covalent interactions, termed "molecular glues",[20] provide an efficient scaffold for biomolecular adhesion[21] that have been useful to tailor various natural processes including protein–protein interactions,[22,23] protein–ligand interactions,[24] enzyme inhibition,[25,26] viral inhibition[27] and actomyosin sliding motion[21] in a site-selective manner. However, the utility of such molecular glues in the augmentation of the activity of biocatalytic cascades is non-existent. Further, the temporal modulation of the biocatalytic cascades using such molecular glues would provide a biomimetic scaffold to design effective therapeutics and mimic the natural biochemical processes.

Utilizing the principles of systems chemistry, synthetic materials have been introduced to mimic the temporal regulation of biocatalytic reactions and biological processes with significant success.[9,28–30] For example, attempts have been made to drive transient assemblies through catalytic reactions[31] and hydrolytic cleavage of peptides, leading to the temporal formation of fibers.[32] Furthermore, the growth and division of

Materials Research Centre, Indian Institute of Science, C.V. Raman Road, Bangalore 560012, Karnataka, India. E-mail: subinoy@iisc.ac.in; Tel: +9180-22932914

† Electronic supplementary information (ESI) available: Synthesis and characterization data of C_nGua and spectroscopic data, additional experimental data of UV-vis, fluorescence, SEM and ITC, Fig. S1–S32 and Table S1. See DOI: https://doi.org/10.1039/d3sc00195d

protein fibrils in coacervates using guanosine triphosphate,[33] light-responsive self-assembly of micro/nanosystems,[34,35] pH-responsive assembly of amphiphiles into nanozyme,[36–38] seeded supramolecular polymerization into chiral assembly[39] and ATP-driven transient nanoreactors to regulate chemical reactions[40] demonstrated dynamic and dissipative processes mimicking cell biology. Various synthetic analogs achieving structural diversities and functions have been introduced including coacervates,[41] emulsions,[42] hydrogels,[43] nanoreactors,[44] molecular motors,[45] polymersomes[46,47] and steady-state supramolecular polymers.[48] There have also been significant advances in developing chemical and biological microreactors for cascade reactions[49–51] using synthetic compartments.[52] Use of diverse types of chemistries has created a repertoire of complex biomimetic systems under dissipative conditions such as enzyme-catalyzed pH cycles for the transient control of polymer fluids[53] and breathing microgels,[54] carbodiimide for self-selection of the primitive reaction network,[55] thiols for self-replicating micelles,[56] and DNA for constructing nanodevices for drug release and reaction networks.[28,57,58] While these dissipative molecules provide a structural component for generating the transient phases, utilization of the building blocks to perform biomolecular functions in the time domain would further enrich our understanding of systems chemistry and produce effective biomimetic scaffolds including molecular adhesives.

In the present study, we introduce a dissipative molecular glue based on a vesicular system (called VesiGlue) comprising a cationic surfactant with guanidinium headgroup and ATP as a capping agent, which allows effective adhesion for enzymes. Notably, ATP here serves the dual role of structure and function: (i) to present the essential structural component for the transient self-assembly, and (ii) to feature a surface-exposed handle to "glue" the enzymes. Given that CytC binds free ATP in an evolutionarily conserved pocket[59] without affecting its active site, ATP can anchor the protein through the adenosine group. An energy-minimized docking study demonstrated that the nucleotide is favorably positioned in the cleft integrating Arg-91 and Glu-69.[60] The sides of the crevice into which the adenine ring fits are provided by Ala-83, Lys-86, and Asn-70, providing a significant hydrophobic character to the cleft. Moreover, the hydroxyl groups on the ribose of ATP form hydrogen bonds with the carboxyl group of Glu-69. The adenine moiety is reported to feature physiochemical interactions with proteins through various interactions including electrostatic, H-bonding as well as aromatic and other nonpolar interactions.[61] Moreover, CH/π interaction provides a key driving force for the recognition of DNA and RNA molecules by proteins.[62] We demonstrate here that non-covalent interactions between the latched adenine and enzyme efficiently attach the enzyme on the VesiGlue surface, retaining its native tertiary structure. Owing to the increased effective concentration and proximity of the CytC and its substrate on the vesicle surface, the catalytic activity of the templated enzymes and biocatalytic cascades is upregulated significantly. Furthermore, orthogonal catalytic cycles enabling oscillation of the ATP concentration lead to dissociation of the assembled structures, with a concomitant decrease of the enzyme catalysis. However, re-supplying ATP in the VesiGlue system enables activation of the biocatalytic cascades in the time domain. The transient activation of individual enzymes and biocatalytic cascades on a biomimetic molecular glue is unprecedented. Furthermore, the temporal regulation of biocatalytic cascades on the vesicular platform effectively mimics the biological processes of heterogeneous cellular components. Such transient vesicular glues would find important applications in nanomedicines and regenerative medicines by on-demand temporal activation of therapeutic enzymes.

Results and discussion

ATP-driven self-assembled vesicles

We designed a supramolecular system consisting of a long alkyl chain with varying lengths (C_n, $n = 12$, 14, 16, 18) having a guanidinium head group that makes a cationic surfactant, which can bind to ATP resulting in an ATP-presenting VesiGlue surface with the affinity to CytC (Fig. 1a). This platform was utilized to modulate the activity of the enzyme. The positively charged guanidinium headgroup was chosen to bind the triphosphate units of ATP through multivalent salt-bridge interactions (Fig. 1b)[63] in a wide pH range owing to its high pK_a value of 13.6. The C_nGua surfactants were synthesized following the protocol as described in the ESI Fig. S1† and characterized by ^{1}H-NMR, ^{13}C-NMR, and mass spectrometry (Fig. S2a–f†). For the supramolecular system, we explored the ability of C_{16}Gua to form transient assembled structures using ATP as a trivalent capping agent. We utilized ATP to serve three purposes: (i) ATP would provide a multivalent cross-linker, aggregating the surfactants through the favorable guanidinium-phosphate salt-bridge interactions, (ii) enzyme-mediated cleavage of the phosphate bond of ATP would lead to its consumption, destabilizing the assemblies, and (iii) the adenine group would act as a glue for proteins. The multivalent interaction between ATP and C_nGua was confirmed using ^{31}P NMR. The significant upfield chemical shift values of the α-P from −11.06 to −11.53, β-P from −22.78 to −23.06 and γ-P from −10.7 to −11.08 of ATP (Fig. 1c) in the presence of C_{16}Gua shows the molecular recognition between the phosphates of ATP and guanidinium units.[64] The NMR spectra also demonstrate the stability of phosphates in the presence of ligands as the peaks do not diminish.

The molecular recognition of C_nGua and ATP leads to discrete aggregates in solution owing to organization of molecules *via* hydrophobic interactions among long alkyl chains and minimized repulsion *via* charge neutralization of the hydrophilic headgroup. The critical aggregation concentration (CAC) of C_nGua/ATP was determined using 1,6-diphenyl-1,3,5-hexatriene (DPH) to investigate the change in aggregation behavior in the presence of ATP.[44] The CAC was found to be approximately 995 μM, 260 μM and 88 μM for C_{14}Gua, C_{16}Gua and C_{18}Gua ligands, respectively (Fig. S3a–c†). While a concentration below the CAC of the ligand prevents its spontaneous self-assembly, supplying energy through a capping agent (ATP) may produce a transiently stable system. The extent of aggregation is directly dependent on the concentration of ATP (Fig. 2a), indicating the presence of intermediate states at sub-

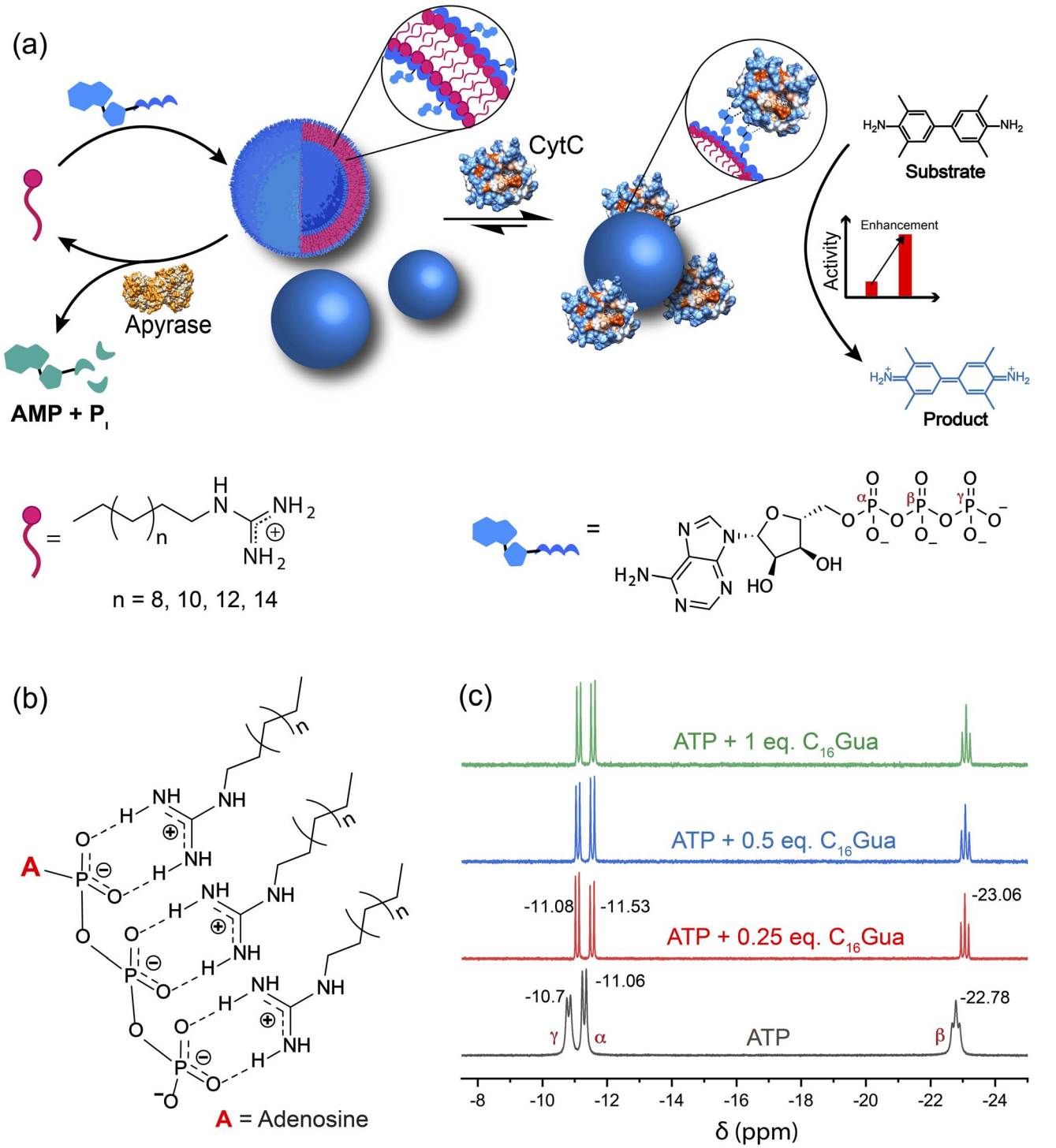

Fig. 1 Design of a supramolecular glue for temporal regulation of enzyme activity. (a) Schematic representation of the transient assembly, presenting non-covalently bound peripheral proteins. The guanidium containing amphiphile and ATP make bilayer vesicular supramolecular assemblies (named VesiGlue), which are disrupted by apyrase enzyme producing the monomers. The VesiGlue binds CytC on the surface and causes amplified biocatalytic activity. (b) Schematic of multivalent salt-bridge interactions between the phosphates of ATP and guanidinium units of the ligand (C_{16}Gua) demonstrating one molecule of ATP interacts with three molecules of C_{16}Gua. (c) ^{31}P NMR spectra (400 MHz) of ATP titrated with different equivalents of C_{16}Gua, showing the interactions involved.

saturation concentrations. Moreover, both the fluorescence (Fig. 2a) and absorbance (Fig. S4†) of DPH dye initially increased, which plateaued at an ATP concentration one third that of C_{16}Gua. Therefore, the transiently assembled structures are produced under saturation conditions of 1 : 3 ATP : C_{16}Gua ratio (henceforth known as C_{16}VesiGlue) irrespective of the total

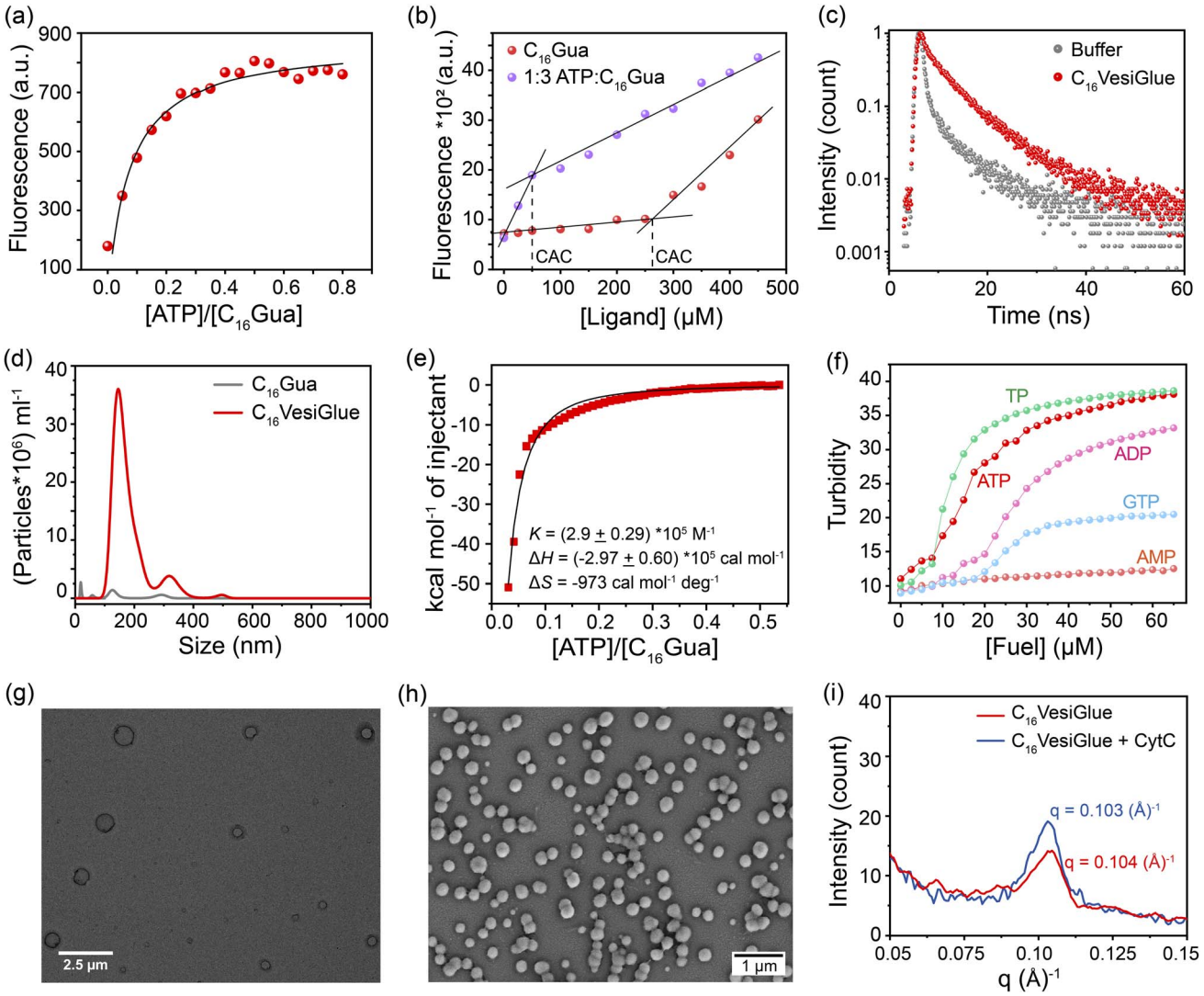

Fig. 2 Fabrication and characterization of ATP-assisted VesiGlue. (a) Fluorescence intensity at 428 nm with increasing concentration of ATP in an aqueous buffered solution containing 100 μM of C_{16}Gua and 2.5 μM of DPH, suggesting the binding ratio of ATP : C_{16}Gua 1 : 3 (named C_{16}-VesiGlue). The black line represents non-linear fitting to guide the eye. au, arbitrary units. (b) CAC of C_{16}Gua *vs.* 1 : 3 ATP : C_{16}Gua. Experimental conditions: [HEPES] = 1 mM, pH 6.0, [DPH] = 2.5 μM, T = 25 °C, Excitation wavelength = 355 nm and Emission wavelength = 428 nm. (c) Time-domain intensity decay of DPH dye in aqueous buffer and in the presence of C_{16}VesiGlue excited using a 375 nm laser, exhibiting an increased lifetime of the hydrophobic dye upon interaction with C_{16}VesiGlue. Normalized intensity is plotted against time. (d) Nanoparticle tracking analysis (NTA) of C_{16}VesiGlue in buffer showing the particle size distribution, compared with C_{16}Gua alone. (e) ITC data demonstrating the thermodynamics of C_{16}VesiGlue formation. ITC measurements were performed by titrating ATP into 100 μM C_{16}Gua (HEPES, 1 mM, pH 6) and fitted to a non-competitive one-site binding model. (f) Turbidity measurements showing assembly formation using 100 μM C_{16}Gua with increasing concentrations of various phosphate analogues including ATP, TP, GTP, ADP and AMP in buffer. Turbidity was calculated by measuring the absorbance at 500 nm, where none of the components absorb. (g) Representative negatively stained TEM image of C_{16}VesiGlue. The higher contrast at the boundary indicates bilayer formation. (h) Representative SEM image of C_{16}VesiGlue structures. (i) SAXS pattern of C_{16}VesiGlue alone and CytC bound structures.

concentration of C_{16}Gua (Fig. S5†), suggesting the assembly formation through the multivalent interactions between triphosphate of one ATP molecule and three molecules of the C_{16}Gua ligand. The fluorescence spectra of DPH at 1 : 3 ATP : C_{16}Gua are shown in Fig. S6,† where an 8-fold enhancement in fluorescence of DPH can be observed upon ATP addition to C_{16}Gua. Furthermore, the CAC of the system estimated with 1 : 3 ATP : C_{16}Gua at different concentrations showed a 5.2-fold reduction to 50 μM (Fig. 2b). A smaller CAC value in the presence of ATP indicates the gain in the stability of the aggregates.[40,44] Accordingly, the average fluorescence lifetime (τ) of DPH showed a substantial increase from 3.93 ns to 5.83 ns upon ATP addition, which indicates localization of the fluorophore in a structured apolar environment of the C_{16}VesiGlue aggregates (Fig. 2c).[44] Likewise, the overall surface charge (zeta potential) of the C_{16}VesiGlue decreased significantly from the C_{16}Gua ligand alone (Fig. S13†). The C_{16}VesiGlue formed within 10–15 min as demonstrated by the kinetics (Fig. S7†).

Next, we investigated the nature of the aggregates and their formation thermodynamics. Initially, we used nanoparticle tracking analysis (NTA) as a robust approach to visualize and track individual colloidal particles in the liquid phase.[65] NTA analysis showed the size distribution of the maximum number of well-defined aggregates to be in the range of 150–250 nm at the 1 : 3 stoichiometric ratio of ATP : C_{16}Gua (Fig. 2d), which is supported by the dynamic light scattering (DLS) measurements showing the average hydrodynamic diameter to be ~250 nm (Fig. S8a†). The thermodynamics of the C_{16}VesiGlue assembly formation studied by isothermal titration calorimetry (ITC) showed an exothermic binding with a strong affinity of $\sim 10^5$ M^{-1}. Furthermore, the molar ratio of ATP to C_{16}Gua was determined to be 1 : 3 by ITC, supporting the binding stoichiometry determined by the spectroscopic studies. Besides, the large negative ΔH value indicates the assembly process to be enthalpy driven (Fig. 2e). Notably, the obtained aggregates were stable for more than 24 h, as revealed by the turbidity measurements (Fig. S9†). The unaltered size of the assembly even after 28 h further underpins the stability of the VesiGlue (Fig. S10†). The longer stability of the aggregates further supports the formation of vesicles, in contrast to similar charge-based coacervates that tend to aggregate within 6–12 hours, with less stability.[66] Significantly, the formation of C_{16}VesiGlue in the presence of biological concentration of NaCl (150 mM) demonstrates considerably high strength of the salt-bridge interactions between triphosphates and guanidinium (Fig. S11†).

To assess the influence of different phosphate analogues with varied valency, we studied the aggregation behavior of C_{16}Gua in the presence of adenosine monophosphate (AMP), adenosine diphosphate (ADP), guanosine triphosphate (GTP) and sodium triphosphate (TP). An apparent decrease in the CAC could be observed along with an increase in the turbidity (at 500 nm) of the solution for all the phosphate analogues (Fig. 2f). Similar to ATP, the triphosphate containing molecules exhibited plateaued turbidity at an XTP/C_{16}Gua (X = G, sodium) stoichiometric ratio of 1 : 3, whereas diphosphate containing ADP exhibited saturation at a ratio of 1 : 2. However, the monovalent AMP did not form any assembly (Fig. 2f), validating the importance of multivalent binding in generating the assembled structures. Next, we compared the GTP/C_{16}Gua assembly with that of ATP/C_{16}Gua to gain insight into the different assemblies formed by two nucleotides. The fluorescence intensity of the encapsulated DPH was almost similar (Fig. S12a†), indicating similar dye encapsulation efficiency of the ATP and GTP systems and utilization of all the C_{16}Gua for vesicle formation. However, GTP/C_{16}Gua assembly exhibited lower turbidity, which depends on different factors including the number of particles, the size of the vesicles and their bilayer thickness.[67] The NTA analysis showed that the concentration of vesicles formed at the 1 : 3 stoichiometric ratio of ATP : C_{16}Gua (2.91×10^9 particles per mL, Fig. S12b†) is ~6.3 fold more compared to GTP : C_{16}Gua (4.61×10^8 particles per mL, Fig. S12b†). Moreover, the GTP-assisted assembly generates larger vesicles (190 nm, Fig. S12c†) than that of the ATP-assisted assemblies (150 nm, Fig. 2d). Interestingly, the bilayer thickness of ATP/C_{16}Gua vesicles (Fig. 2i) decreased from ~6 nm to ~3 nm in the case of GTP/C_{16}Gua vesicles (Fig. S12d†) as evident from the small angle X-ray scattering (SAXS) results. The difference in the assembly behaviour of the two nucleotides can be attributed to the stronger and larger number of intermolecular hydrogen bonds for ATP than that of GTP.[39,68]

To further elucidate the size and morphology of the C_{16}-VesiGlue aggregates, various analytical techniques were utilized. Transmission electron microscopy (TEM) and field emission scanning electron microscopy (FESEM) images demonstrate that the aggregates present a vesicular morphology with diameters 150–250 nm (Fig. 2g and h, respectively). Notably, the TEM images showed a higher contrast at the boundary of the spherical assemblies that indicates the presence of bilayer structures.[44] However, the C_{16}Gua alone at the same concentration did not produce any assembly (Fig. S14†). Interestingly, it formed micellar structures with a size of ~30 nm above the CAC, as verified by DLS (Fig. S15†) and TEM (Fig. S16†) results. To visually observe the distribution of a hydrophobic fluorophore (Nile red) in the assembled structures, the sample was 3D scanned by confocal laser scanning microscopy (CLSM) (Fig. S17†). Although the size of the assemblies falls below the resolving power of CLSM, the accumulation of Nile red dye in the apolar bilayer of the C_{16}VesiGlue allowed the structures to be detected. It can be observed that the dye gets entrapped within the hydrophobic domain of the spherical vesicles (Fig. S17†). A dye (calcein) release assay further confirmed the vesicle formation. Calcein undergoes self-quenching at high concentrations in the lumenal space of synthetic vesicles but shows a dramatic increase in fluorescence emission upon membrane disruption.[69] A non-ionic surfactant Triton X-100 was used to permeabilize the VesiGlue, resulting in calcein release. Complete vesicle disruption corresponding to the 100% dye release was achieved by 350 μM of Triton X-100 (Fig. S18†) validating the formation of vesicles using C_{16}Gua-ATP. The vesicle wall thickness was determined by the SAXS experiment using Bragg's equation ($d = 2\pi/q$),[70,71] with a derived value of ~6 nm (Fig. 2i). Moreover, increasing NaCl concentration led to enhanced fluorescence of the hydrophobic DPH probe entrapped in the hydrophobic part of the C_{16}Gua and ATP/GTP/TP assemblies (Fig. S19†). This observation further ascertains the bilayer structure of VesiGlue since the typical bilayer membrane rigidity increases with increasing salt concentration.[72] Therefore, the stability coupled with the analytical results support the formation of self-assembled bilayer vesicles *via* strong non-covalent salt-bridge interactions between guanidinium and triphosphate.

"Vesicular glue" for molecular recognition of proteins

Modulation of the enzymatic activity of proteins by synthetic materials is an important aspect of protein-based bioengineering as well as to understand the diverse range of reactions inside the cells and predict the metabolism of living things.[73] Therefore, we investigated the possibility of temporally regulating the activity of an enzyme using the self-assembled C_{16}-VesiGlue. Given the importance of CytC enzyme in the electron

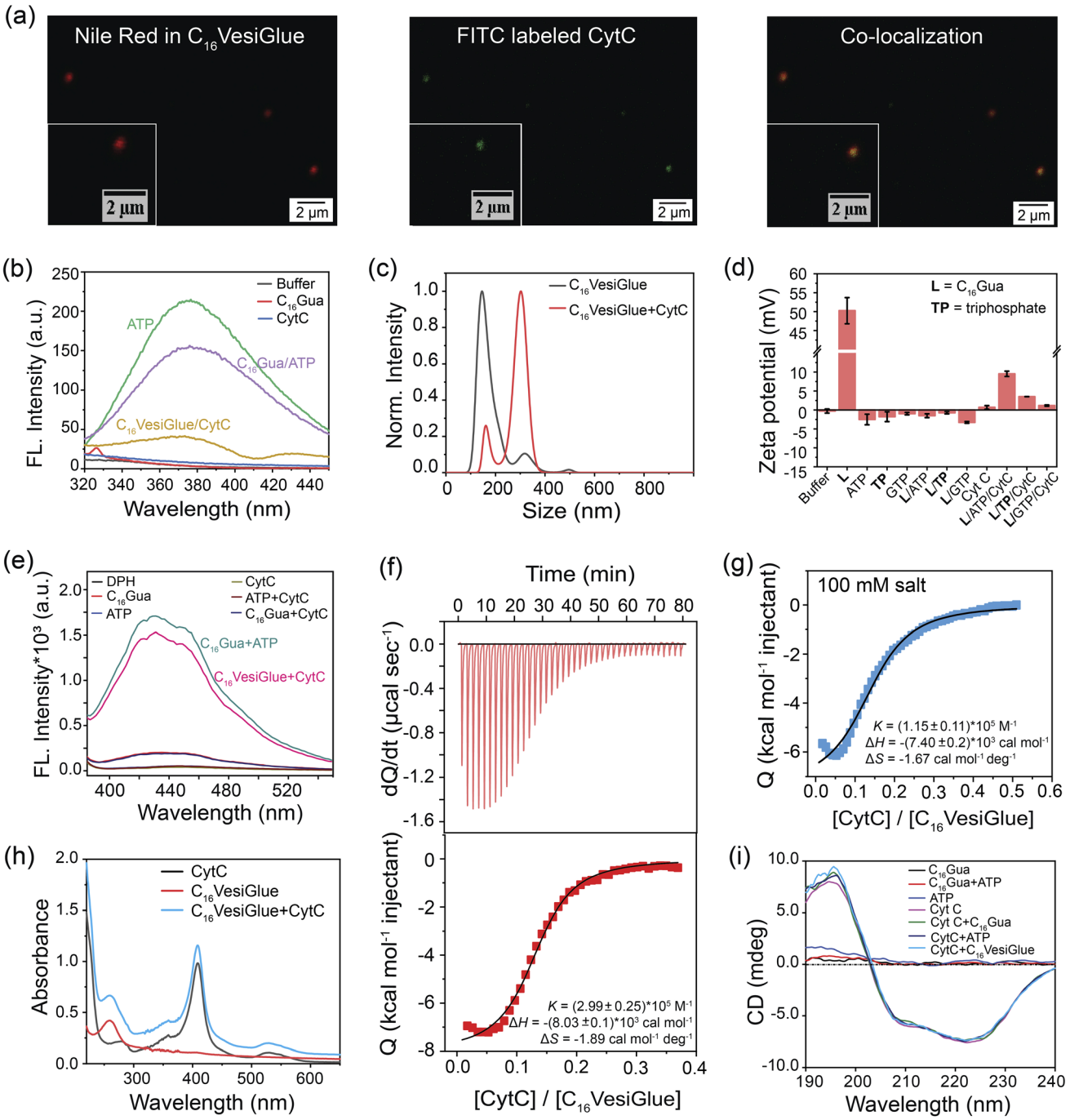

Fig. 3 VesiGlue for the molecular recognition of proteins. (a) Representative CLSM images showing Nile red stained C_{16}VesiGlue (red fluorescence), FITC-labeled CytC (green fluorescence) and co-localized (orange) ATP-templated structures. (b) Fluorescence intensity of ATP (green) at $\lambda_{exc.}$ 260 nm upon interaction with C_{16}Gua forming VesiGlue (purple) and CytC (yellow). (c) NTA measurements of C_{16}-VesiGlue (black) with CytC glued on the surface (red). (d) Zeta potential of XTP/C_{16}Gua (X = G, sodium) systems (1 : 3 molar ratio) in the presence of CytC in buffer. $n = 3$ technical replicates, mean ± SD for all the studies. (e) DPH dye leakage experiment. The fluorescence intensity of DPH ($\lambda_{exc.}$ 355 nm) containing assembly was measured upon CytC addition. (f) Top: Raw ITC thermogram of CytC titrated into C_{16}VesiGlue in 1 mM HEPES buffer (pH 6), exhibiting exothermic peaks. Bottom: Integrated heat flow signals as a function of CytC/VesiGlue molar ratio. The best fit was obtained by a single-site non-competitive binding model, demonstrating a highly favorable binding affinity. (g) Integrated heat flow obtained from the ITC thermogram for the titration of CytC into C_{16}VesiGlue in the presence of 100 mM salt concentration. (h) UV-vis spectral scan of CytC (black), VesiGlue (red) and CytC in the presence of VesiGlue (blue) shows the unaffected heme centre of CytC upon binding to VesiGlue. (i) CD spectra of CytC in the presence of VesiGlue and the appropriate controls demonstrating the stability of the secondary structure of CytC.

transport chain,[74] we studied the peroxidase activity of CytC templated on the vesicle surfaces. First, CLSM imaging was performed using the Nile red-entrapped C_{16}VesiGlue and FITC-tagged CytC to determine if CytC is "glued" to the C_{16}VesiGlue surface. As illustrated in Fig. 3a, the green fluorescence of FITC-labelled CytC is decorated on the C_{16}VesiGlue surface, whereas distinguishable fluorescent structures were never observed in the absence of ATP. The SAXS pattern for the CytC@VesiGlue showed an insignificant shift of 0.001 $(Å)^{-1}$, indicating that the vesicle wall thickness does not change upon binding the protein (Fig. 2i). Therefore, CytC should be bound to the outer surface and not intercalated inside the hydrophobic domain of the vesicle. The gluing of CytC was further probed by the native fluorescence of ATP that decreases upon interaction with another molecule.[75,76] The ATP fluorescence at 360 nm decreased 1.4-fold upon the addition of C_{16}Gua to ATP at the CAC. The fluorescence emission of ATP further decreased with the addition of CytC (Fig. 3b), indicating favorable biochemical interaction between CytC and ATP present on the C_{16}VesiGlue surface. Furthermore, the increased average particle size (Fig. 3c) from 180 nm to 300 nm observed in NTA upon the addition of CytC further suggests its templation on the surface of C_{16}VesiGlue. Formation of the protein corona over the VesiGlue surface results in the crowding of a few vesicles *via* aggregation resulting in increased size, similar to that observed for liposomal platforms.[77] The result was further supported by DLS measurements (Fig. S20†), wherein the hydrodynamic diameter was found to be ~450 nm. Similarly, the Zeta potential of the C_{16}VesiGlue changed from −0.43 mV to +9.53 mV upon the addition of CytC (Fig. 3d). Zeta potential being average surface charge of the particles, the increased positive charge indicates peripheral association of CytC on the bilayer vesicles. Furthermore, we studied the integrity of the VesiGlue membrane in the presence of CytC, as different biomolecules including proteins can penetrate and/or disrupt cell/organelle membranes.[78] A dye leakage assay was performed using a DPH-intercalated VesiGlue bilayer. The hydrophobic DPH dye causes enhanced aggregation-induced fluorescence in the hydrophobic bilayer of VesiGlue, which should be quenched upon membrane disruption. Incubation of CytC with C_{16}VesiGlue did not produce a significant change in the fluorescence of DPH (Fig. 3e), suggesting high stability of the VesiGlue membrane and peripheral anchorage of CytC.

The specific molecular recognition of CytC by C_{16}VesiGlue has been proven *via* ITC measurements as well as later by the activity assays. ITC study showed that the CytC interacts with C_{16}VesiGlue with a binding affinity of 2.99×10^5 M^{-1} (Fig. 3f), which is ~3-fold stronger than the affinity of CytC with TP-templated aggregates (1.18×10^5 M^{-1}) (Fig. S21a†). This demonstrates the importance of the adenine unit of ATP for the specific non-covalent binding with the amino acids of CytC *via* supramolecular interactions.[61] The most important factors contributing to the negative values of enthalpy and entropy, and hence to the stability of protein glued on C_{16}VesiGlue, are van der Waals interactions. The binding affinity of CytC with free ATP was 6.59×10^4 M^{-1}, which is ~4.5-fold weaker than with the ATP templated on C_{16}VesiGlue (Fig. S22†), possibly due to a multivalent effect.[79–81] Further, the binding affinity of CytC with GTP-assisted aggregates was less (3.7×10^4 M^{-1}) compared to that of ATP (Fig. S21b†). The result indicates the specific binding of the adenine group with the protein mainly *via* electrostatics and H-bonding interactions.[61] Furthermore, the protein was still bound on the C_{16}VesiGlue surface at a salt concentration of 100 mM with a binding affinity of 1.15×10^5 M^{-1} (Fig. 3g), demonstrating the nature of interaction not to be purely electrostatics through the phosphate of ATP and cationic amino acids on the protein. It is worth noting that control studies with TP-templated vesicles did not show any binding with CytC in 100 mM NaCl (Fig. S23†) while keeping the vesicular assembly intact (Fig. S24†), which shows CytC binding through electrostatics only. These studies indicate the important role of the nucleosides in binding CytC through various non-covalent interactions in addition to electrostatics.

The impact on the native structure of the protein upon binding with C_{16}VesiGlue was monitored using UV-vis spectral scans that can detect any change in the micro-environment near the heme center. In addition to the peak at 280 nm, CytC has three characteristic peaks centered at 360 (δ band), 409 (Soret band), and 530 nm (Q band).[82] These bands remain unaffected upon attachment to C_{16}VesiGlue (Fig. 3h), suggesting that the active site of CytC remains intact. The integrity of the protein structure was further assessed by circular dichroism (CD) that showed no significant deviation or alteration of the ellipticity corresponding to the characteristic peaks at 208 and 222 nm of the protein (Fig. 3i). Therefore, the secondary structure of CytC remained unchanged in the presence of the self-assembled C_{16}VesiGlue. While the earlier reported micellar systems with exposed charged groups[83] and amphiphilic homopolymers[84] showed alteration of CytC native structure, the VesiGlue system provides a non-denaturing platform that retains the protein structure. The intact secondary structure of the protein also indicates that CytC latches onto the surface of the assembly rather than being embedded within the hydrophobic domain.[83] Taken together, all these results coupled with (a) the favorable interaction between the neutral/slightly negative C_{16}VesiGlue and cationic protein, (b) CytC possessing a conserved ATP binding pocket,[59] and (c) lesser binding of the negative controls of GTP, AMP, triphosphate at their corresponding CACs, point at the nature of gluing interaction being multivalent non-covalent interaction between the exposed ATP on C_{16}VesiGlue surface and CytC.

Amplified enzyme activity on VesiGlue

Given the retention of CytC native structure, we investigated whether the enzymatic activity of the enzyme is modulated on the C_{16}VesiGlue surface. The peroxidase activity of CytC was studied by monitoring the rate of conversion of the substrate 3,3′,5,5′-tetramethylbenzidine (TMB) to 3,3′,5,5′-tetramethylbenzidine diamine (TMB_{ox}) in the presence of oxidant H_2O_2. As observed from Fig. 4a, ATP alone increases the specific activity of CytC by 3.2 fold, which got further enhanced by 8.4 fold when CytC is bound to ATP on the vesicle surface. Interestingly, the same equivalents of TP-assisted assembly did not

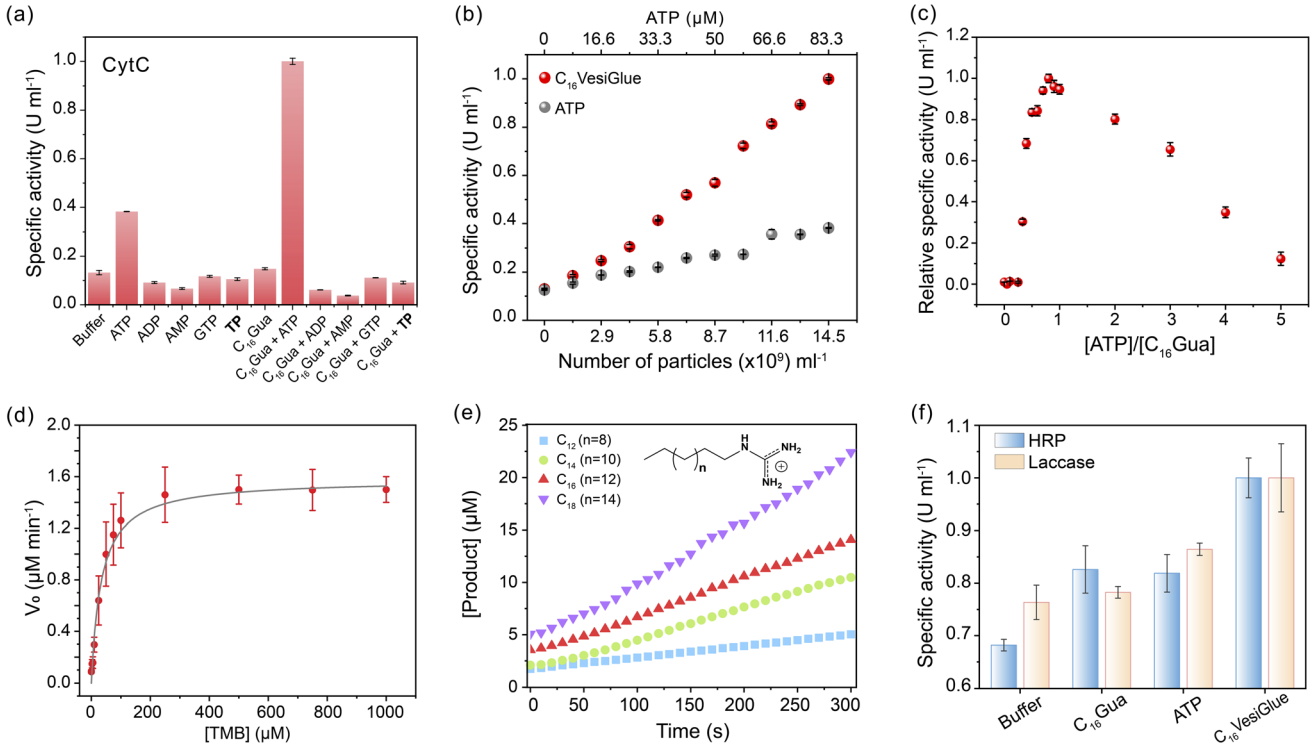

Fig. 4 Augmented enzyme activity on VesiGlue. (a) The relative specific activity of CytC in the presence of the assemblies formed *via* different phosphate analogues (ATP/ADP/AMP/TP/GTP) and C_{16}Gua in 1 : 3 molar ratio. The controls of the phosphate analogue alone do not produce amplified enzyme activity except ATP. (b) The specific activity of CytC in the presence of varying C_{16}VesiGlue concentration (red) *vs.* only ATP (grey). The C_{16}VesiGlue concentration (particles per mL) was measured by NTA. (c) The relative specific activity of CytC in the presence of varying ATP equivalents to C_{16}Gua. (d) The Michaelis–Menten plot was derived for the different concentrations of TMB. (e) Rate of the product (TMB_{ox}) formation by CytC anchored on VesiGlues formed with a varying chain length of ligand C_nGua (n = 12, 14, 16, 18). Experimental conditions: HEPES buffer 1 mM pH 6, [ligand] = 100 μM, [ATP] = 33 μM, [CytC] = 0.5 μM, [TMB] = 100 μM and [H_2O_2] = 2 mM. (f) Specific activity of HRP and Laccase measured in the presence of C_{16}VesiGlue using the substrates TMB and ABTS, respectively, signifying the versatility of the system in catalyzing the enzyme's activity. n = 3 technical replicates, mean ± SD for all the results.

exhibit any enhancement of the CytC peroxidase activity (Fig. 4a), clearly demonstrating the essence of the adenine group of ATP that interacts with CytC *via* non-covalent interactions including electrostatic, H-bonding, and aromatic interactions.[61] Notably, GTP-driven assemblies failed to enhance the enzyme activity (Fig. 4a), which supports the importance of adenine in the molecular recognition of the enzyme on the C_{16}VesiGlue surface. Although the assembly containing a hydrophobic compartment is formed in the case of C_{16}Gua with different triphosphate analogues (TP and GTP) as well, the lack of CytC activity enhancement in these assemblies clearly demonstrates the importance of ATP as a recognition site for CytC.

The augmented CytC activity on C_{16}VesiGlue was postulated to arise from the increased local concentration of CytC and substrate on the vesicle surface[85] and increased affinity of CytC to C_{16}VesiGlue. The localized density of enzymes in a given volume dramatically increases when multiple enzymes are attached to a single particle *versus* a free enzyme. Also, we observed TMB substrate binding to the vesicle surface (Fig. S25†), along with a stabilizing effect of the vesicle. The increased localized concentration of CytC and the substrate on C_{16}VesiGlue increase the collision frequency of the substrates with the enzymes resulting in the acceleration of the catalyst activity.[86] Further, the favorable position of adenine aromatic ring[60] above the heme unit of CytC facilitates proton transfer from H_2O_2 to the nucleobase (Fig. S26a†), which leads to accelerated hydroxyl radical generation and a stabilized intermediate of TMB oxidation product (Fig. S26b†). The higher affinity of CytC to the VesiGlue possibly aids in this process showing the highest stability of the TMB radical cation intermediate.[87]

The activity of CytC@C_{16}VesiGlue is enhanced linearly with the increasing concentration of the C_{16}VesiGlue particles (Fig. 4b), validating the templation effect of the vesicular glue. The augmented activity of CytC due to gluing on the VesiGlue was further confirmed using competitive binding at higher equivalents of ATP. While the specific activity of CytC was enhanced at 1 : 3 ATP : C_{16}Gua stoichiometry, it was saturated at ~7 equivalents of ATP (Fig. 4c). Higher equivalents of ATP lead to a gradual decrease in activity, ultimately reaching activity similar to that of the non-templated CytC, suggesting the dissociation of CytC from VesiGlue surface due to competitive binding. Further, the catalytic activity of CytC was observed to increase with reaction time (Fig. S27†). To understand the kinetic behavior of the system, the catalytic activity of

CytC@C_{16}VesiGlue was measured at different concentrations of TMB (Fig. S28a†). The kinetic pattern suggests that the CytC glued on C_{16}VesiGlue follows the Michaelis–Menten model (Fig. 4d). The kinetic parameters were determined from the Michaelis–Menten plot and are shown in ESI Table 1.† The Michaelis–Menten plots for CytC alone and CytC with ATP are shown in Fig. S28 (b and c).† The Michaelis constant (K_M) value of 44.16 μM for native CytC reduced to 33.97 μM when bound to C_{16}VesiGlue, suggesting the substantially enhanced substrate affinity of the enzyme glued on C_{16}VesiGlue. The high k_{cat} of CytC@C_{16}VesiGlue indicates higher catalytic efficiency compared to the unbound CytC, which can be further increased upon increasing the concentration of the C_{16}VesiGlue particles as evident from the experiment in Fig. 4b.

Further, we studied the effect of the alkyl chain length of the guanidinium-terminated ligands in modulating the activity of CytC. For VesiGlues of varied alkyl chain lengths of C_{12}, C_{14}, C_{16}, and C_{18}, increased activity was observed (Fig. 4e). Consequently, a 6-fold difference in specific activity was observed between the C_{12} and C_{18} ligands, which could be due to the significant size difference between the assemblies formed by the two (Fig. S8b†). To test if any cationic surfactant forms the vesicles and upregulates enzyme activity, we tested the quaternary ammonium group bearing cetyltrimethylammonium chloride (CTAC) and ATP pair that would interact through electrostatics. It was found that the CytC activity enhancement by CTAC/ATP structures was about 2.5-fold less than that with the C_{16}-VesiGlue (Fig. S29†). Therefore, the salt bridge interaction between guanidinium and phosphates of C_{16}VesiGlue provides a stronger and selective non-covalent bonding than the simple electrostatic interaction between the quaternary ammonium group and phosphates in the CTAC/ATP vesicles. Next, the specific activities of horseradish peroxidase (HRP) and laccase enzymes were measured to examine the versatility of the template effect of the system (Fig. 4f). Activity of HRP was monitored by the extent of oxidation of TMB as a substrate. The specific activity of HRP was enhanced by 1.5 fold in the presence of C_{16}VesiGlue compared to that of ATP only. ABTS was used as a substrate to study the oxidase-like activity of laccase decorated on the C_{16}VesiGlue. It was observed that laccase activity enhanced by 1.3-fold in the presence of C_{16}VesiGlue, which further proves the versatility of the system. Altogether, vesicular glue provides a robust and generalized platform to augment the catalytic activity of different enzymes.

Cascade reactions in the VesiGlue system

A cascade reaction is a multistep chemical reaction in which a substrate is transformed into a product that becomes a substrate for the subsequent reaction.[88] Biomolecular cascades play a central role in multiple biological processes including cell response towards a stimulus, initiation of blood coagulation, production of carbohydrates through photosynthesis, *etc.*[89] We demonstrate a two-step cascade reaction using glucose oxidase (GOx) and C_{16}VesiGlue templated CytC. GOx is an oxidoreductase enzyme that catalyzes the aerobic oxidation of glucose to gluconic acid with the simultaneous formation of H_2O_2, initiating the second catalytic reaction of TMB in the presence of CytC (Fig. 5a). ITC study showed that GOx interacts with C_{16}VesiGlue with a binding affinity of 4.60×10^4 M^{-1} (Fig. S30†), which is significant to be bound on the vesicle surface. For the two-step cascade reaction, the activity was monitored by adding the substrate glucose along with TMB as the chromogenic substrate for the terminal cascade reaction, producing a greenish-blue product (Fig. 5a). The catalytic activity of the cascade reaction was enhanced as the concentration of GOx enzyme was increased, monitored from the absorbance of oxidized TMB at 650 nm (Fig. 5b and c). Moreover, the kinetics of oxidized TMB product formation was monitored by UV/vis spectroscopy (λ_{max} = 650 nm, Fig. 5d) showing the increased product formation with time. The activity of the cascade by GOx/CytC/C_{16}VesiGlue was found to be 0.223 ± 0.0014 μM min^{-1} with 0.3 nM of GOx and 5 mM of glucose, plotted as relative specific activity of CytC (Fig. 5e).

Interestingly, cascade activity in the presence of C_{16}VesiGlue was 6.5-fold higher compared to the controls of free GOx/CytC diffusional mixture at the same concentration. However, separately used CytC/C_{16}VesiGlue and GOx/C_{16}VesiGlue did not show any noticeable activity (Fig. 5e), indicating the crucial role of the VesiGlue templated cascade reaction in producing the oxidized product. The effect of pH change induced by GOx and glucose reaction around the experimental concentrations was monitored (Fig. S31†). The change in pH of the medium was very minimal that did not disrupt the C_{16}VesiGlue vesicles as evidenced by the insignificant change in solution turbidity. Moreover, the GOx/CytC/C_{16}VesiGlue cascade reaction showed a linear dependence on the substrate (glucose) concentration (Fig. 5f). Besides, the linear standard curve showed a detectable signal even at a concentration of 10 μM (3 × standard deviation of the blank), demonstrating high sensitivity of the platform toward glucose. The binding affinities of both the cascade partner enzymes with VesiGlue were significant, which may suggest colocalization of the enzymes on the vesicle surface. Overall, these results indicate that "gluing" CytC on the vesicle surface helps facilitate the cascade reaction *via* increasing the effective local concentration of the substrates.[85]

Temporal control of enzyme activity and biocatalytic cascades

We tested the efficacy of VesiGlue to regulate the augmented enzyme activity in the time domain as long as the ATP is present, emulating biological processes such as signal transduction, transport, and cell division.[1,90] Given the ATP-dependent VesiGlue formation, we hypothesized that oscillation of the ATP concentration could switch between two distinct, transient states in a recyclable, dissipative process with a controllable lifetime. To achieve the goal, another cycle requires to be introduced that utilizes the ATP followed by its conversion to inactive waste with concomitant destabilization of the system.[30] We achieved this cycle using potato apyrase (PA) enzyme, which hydrolyses ATP to adenosine 5′-monophosphate (AMP) and two molecules of orthophosphate (P_i). The produced AMP and P_i with a monovalent phosphate unit do not stabilize the assembly (Fig. 2f), resulting in the disassembly of C_{16}Gua

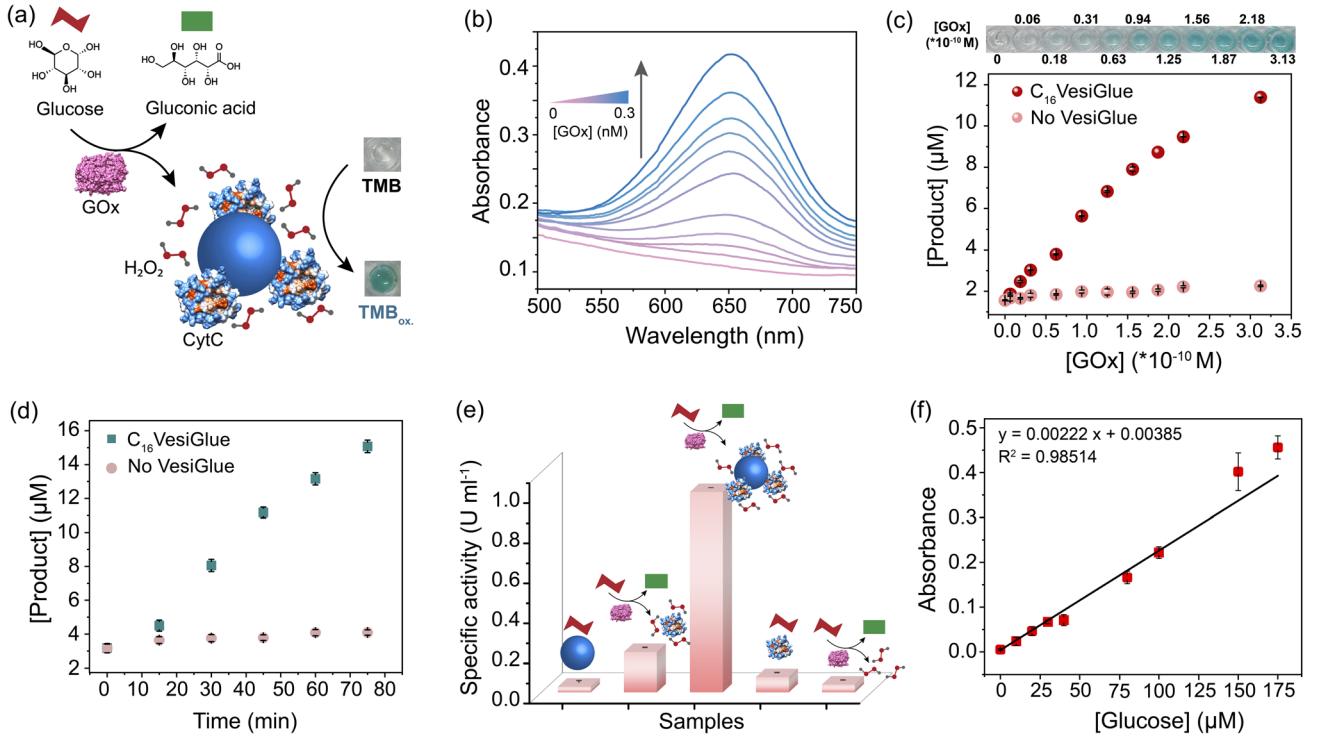

Fig. 5 Cascade reaction in the VesiGlue system. (a) Schematic of a biocatalytic cascade where glucose is oxidized by glucose oxidase (GOx), producing H_2O_2 that serves as the substrate of CytC glued onto VesiGlue. (b) UV-vis traces of oxidized TMB (TMB_{ox}) with increasing GOx concentration, in the catalytic cascade. (c) C_{16}VesiGlue mediated oxidation of the substrate by the biocatalytic cascade. The concentration of TMB_{ox} is measured through the absorbance at λ_{max} 650 nm. Varying concentrations of GOx (0–0.3 nM) in the presence (red) and absence (peach) of C_{16}VesiGlue show the linear dependency on the enzyme concentration. The digital photos above the graph show the color of the TMB_{ox} in presence of C_{16}VesiGlue. (d) Rate of product formation (TMB_{ox}) in the presence (green) and absence (peach) of VesiGlue demonstrating the effect of CytC anchoring on the cascade reaction. (e) Specific activity of CytC under different conditions verifying the role of a complete system in catalyzing the cascade reactions. The shapes of (a) are used that have the same meaning. (f) The GOx/CytC/C_{16}VesiGlue cascade reaction with increasing glucose concentration (0–175 μM). The black solid line represents a linear fit of the data. $n = 3$ technical replicates, mean ± SD for all the studies.

surfactants. In the absence of PA, the fluorescence signal of DPH remained constant in time upon ATP addition to C_{16}Gua, indicating the stability of the VesiGlue under these conditions. However, the presence of different PA concentrations (0–1 U mL^{-1}) led to a decay in fluorescence signal depending on the PA concentration (Fig. 6a) due to the breakdown of the C_{16}-VesiGlue. 1 U mL^{-1} of apyrase could break almost 90% assembly formed by 50 μM C_{16}Gua and 16.6 μM ATP in ~50 min. We studied the oscillatory behavior through fluorescence intensity-time trajectory using DPH dye sequestration in the assembled structures. Consequent resupplying the system with 0.33 equivalent of ATP leads to gradual enhancement of the DPH emission intensity to that of before breakage, suggesting the reformation of the C_{16}VesiGlue (Fig. 6b). After each cycle of PA-mediated cleavage and reproduction, the system did not achieve the initial fluorescence intensity. Accumulation of the byproducts of ATP hydrolysis including AMP and inorganic phosphate (Pi) compete with the VesiGlue formation, which decreases the fluorescence intensity in the subsequent cycles suggesting the competing effect of the byproducts with ATP.[44] The lack of multivalent interactions of ATP in the presence of PA could not induce the vesicle formation as observed from the decreased particles (from 5.8 × 10^9/mL to 7.1 × 10^8/mL) and non-uniform size distribution through NTA study (Fig. 6c). The instability of the assembly could also be visualized by confocal microscopy *via* addition of PA to Nile red entrapped C_{16}-VesiGlue, resulting in decreased particles (Fig. 6d). The results demonstrate the transient formation of vesicle in the presence of ATP as a capping agent. Similarly, the PA-controlled transience of CytC@C_{16}VesiGlue was studied using the modulation of DPH fluorescence. Cleavage of the vesicles by PA with the subsequent addition of 0.33 equivalent of ATP leads to the gradual enhancement of the DPH emission intensity, suggesting the reformation of the VesiGlue, even in the presence of CytC (Fig. 6b). Therefore, the lifetime of CytC bound C_{16}-VesiGlue is efficiently oscillated in this system.

Next, the temporal regulation of enzyme activity on the VesiGlue surfaces was attempted to mimic the adaptive biological systems with temporal control of enzyme activities upon consumption of energy. Specifically, we investigated the activity of the templated enzyme as long as the system stays in the transient state in the VesiGlue form. Regulation of enzymatic activity in the time domain was studied using CytC glued onto the C_{16}Gua/ATP system, and PA to utilize the ATP that leads to disruption of VesiGlue. Given the interference of PA on TMB oxidation, the activity of CytC was measured using a well-known

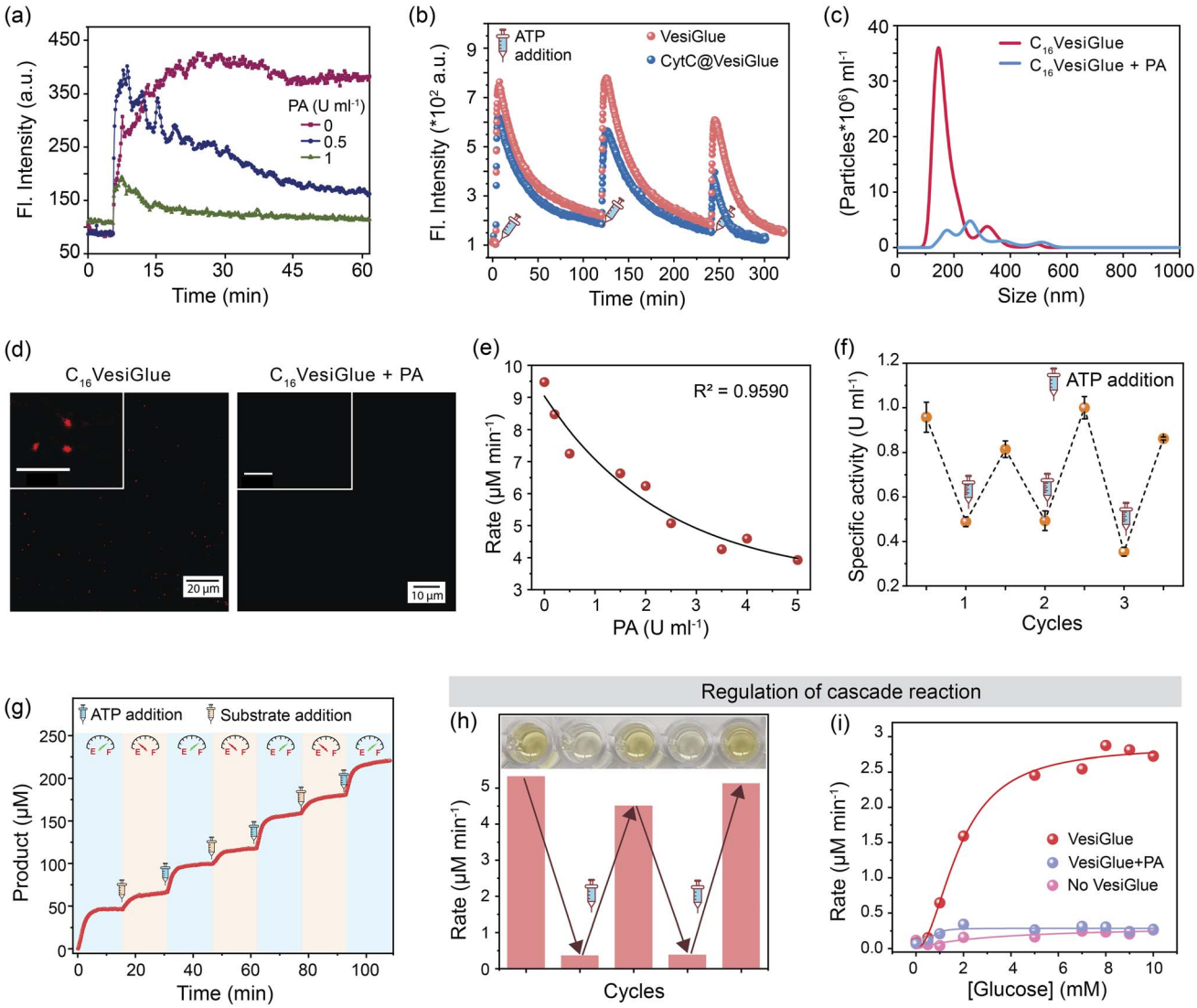

Fig. 6 Temporal control of enzyme activity and biocatalytic cascades. (a) Time-dependent fluorescence of DPH dye at 428 nm following the addition of ATP to C_{16}Gua (1 : 3) and DPH in the presence of different concentrations of potato apyrase. (b) Fluorescence Intensity at 428 nm following three repetitive additions of ATP to a system forming VesiGlue (pink) and CytC@VesiGlue (blue) in the presence of DPH and PA (1 U mL^{-1}). (c) NTA measurement of VesiGlue in the presence (blue) and absence (red) of apyrase (1 U mL^{-1}) where the area under the graph represents the total number of particles per mL. The particle number and uniformity decrease upon PA addition. (d) Confocal images of Nile red (NR) entrapped assembly in the absence and presence of PA (1 U mL^{-1}), disruption of VesiGlue upon PA treatment releases NR leading to the disappearance of red fluorescence. The scale bar of insets is 5 µm. (e) The rate of biocatalytic oxidation by VesiGlue-templated CytC is modulated by the PA concentration. The black line represents exponential decay fitting to guide the eye. (f) Normalized specific activity of VesiGlue-templated CytC measured by the catalyzed oxidation of pyrogallol ($n = 3$ technical replicates, mean ± SD). Temporal regulation of CytC activity was achieved through oscillation of the ATP concentration by the presence of PA and the addition of ATP when the vesicular assemblies are disrupted at 30 min. (g) Time-dependent UV-vis traces at 420 nm (corresponding to purpurogallin formation) with time in the presence of PA. The ATP concentration leads to a higher initial rate of reaction, while the subsequent addition of pyrogallol substrate shows a much slower increase in rate due to free CytC. E and F on the clock represent empty and full ATP levels, respectively. (h) Control of the GOx/CytC/C_{16}VesiGlue cascade reaction *via* ATP-Apyrase feedback control. The image shows the color change upon product formation in the corresponding microwell. (i) Rate of purpurogallin formation in the presence of varying initial substrate (glucose) concentration (0–10 mM). The decrease in the rate of cascade reaction in the presence of PA or without the VesiGlue is independent of the increasing glucose concentration. The lines represent the non-linear fitting to guide the eye.

substrate pyrogallol. The substrate upon catalyzed oxidation in the presence of H_2O_2 converts to purpurogallin and shows a yellow color with $\lambda_{max} = 420$ nm. The augmented specific activity of CytC attached to the VesiGlue was gradually down-regulated as the PA slowly disintegrated the C_{16}VesiGlue, which was dependent on the VesiGlue and PA concentrations (Fig. 6e). Therefore, ATP truly provides the trigger for the amplified activity of the peripheral protein on the vesicular glue. Indeed, each subsequent addition of 0.5 equivalents of ATP led to upregulation of the peroxidase-like activity of CytC to the initial

specific activity. ATP-dependent oscillation was demonstrated for three complete cycles without losing considerable enzyme activity (Fig. 6f), indicating continuous operation as long as the ATP is present. The time-dependent CytC activity regulation over VesiGlue formation and disruption is shown in Fig. 6g. VesiGlue-bound CytC was monitored for its catalytic activity in the presence of PA by adding the substrate pyrogallol. Once PA disrupts the VesiGlue by cleaving the trivalent ATP into AMP, the activity was reduced significantly (pale yellow region of Fig. 6g) due to the unbound CytC in the solution. Interestingly, subsequent replenishment of substrate to the initial concentration did not attain the catalytic rate (V_0, 6.75 μM min^{-1}) same as that of the CytC@VesiGlue system (V_0, 13.23 μM min^{-1}). However, replenishing the system with ATP resulted in enhanced activity (V_0, 11.30 μM min^{-1}) of CytC (light blue region of Fig. 6g) similar to that of the first cycle. We successfully carried out the activity regulation for three continuous cycles without any fatigue. Given the CytC activity enhancement by ATP itself, it was possible to modulate CytC activity using PA, however to a lower extent (~20%) compared to C_{16}VesiGlue (~70%) as demonstrated in Fig. S32.† Therefore, we demonstrated effective modulation of CytC activity on VesiGlue using ATP as a dissipating stimulus. This temporal regulation of enzyme activity underscores the subtle but significant role of the transiently assembled vesicular glue.

Further, we investigated the regulation of cascade reactions on the VesiGlue system, which would be a significant addition to building up the complexity in dissipative synthetic systems. While the two-step cascade reaction using GOx/CytC/C_{16}-VesiGlue system exhibits a faster rate of oxidation in the presence of VesiGlue, the rate decreases by 90% upon the addition of 1 U mL^{-1} PA with sufficient incubation time. Interestingly, the re-enhancement in the rate of purpurogallin formation could be achieved upon successive addition of ATP, thus demonstrating the reversible cycles of enzymatic cascades (Fig. 6h). Besides, a linear dependency between the cascade reaction rate and the substrate (glucose) concentration was observed, which was diminished to the same value as GOx/CytC control upon addition of PA (Fig. 6i). Therefore, we were successful in the proximity-induced augmentation of biocatalytic cascades in the time domain using ATP as a dissipating glue.

Conclusions and future scope

Membrane-bound compartments in the cells require a constant energy supply to arrest the transient state and spatiotemporally control peripheral enzyme functions by oscillating the molecules. Bioinspired transient assemblies presenting peripheral proteins with the ability to regulate amplified activity in response to chemical stimuli would provide adaptive and smart molecular materials. In this study, we demonstrate the generation of peripheral enzymes presenting transient vesicular glue that upregulates the activities of diverse enzymes. Compared to the previously reported traditional dissipative systems utilizing the ATP as a structural component, we showcase, for the first time, that the ATP can perform an active function of attaching proteins on the vesicle surface using multivalent non-covalent salt-bridge interactions. The efficacy of the system was realized in the activation of biocatalytic cascades with augmented enzymatic reactions. Moreover, the VesiGlue shows dissipative behavior in the presence of apyrase enzyme that consumes the ATP. Based on the observation, we successfully constructed a transient vesicular glue that is driven by ATP in the presence of apyrase, with a tunable lifetime. Consequently, temporal regulation of individual enzymes and catalytic cascades is achieved in response to the ATP oscillation. These results present an entirely new way of temporally modulating biocatalytic cascades using a supramolecular vesicular glue, emulating the natural systems. Therefore, we believe that the present generalized approach will allow the development of new life-like systems with time-gated enzyme activity regulation on cellular components including extracellular vesicles.

Beyond the utility of the transient VesiGlue as a model system mimicking the dissipative biological processes, the concept can be extended to expedited chemical synthesis and biomedical applications. For example, directed evolution of proteins against the adenine group or other substituted phosphates would provide specific molecular recognition of therapeutic proteins,[91] with regulated activity in the time domain. Likewise, the transient enzymatic cascades with upregulated activity can potentially have therapeutic applications,[58] such as the temporal control of intracellular signaling agents[92] or the dose-dependent generation of reactive oxygen species as therapeutics.[93] Furthermore, the current study on dissipative vesicles with protein corona shows great promise in providing a delivery vehicle for permeation in cellular organelles and intervening with the cellular processes.

Data availability

The data that support the findings of this study are available from the corresponding author upon reasonable request.

Author contributions

The project concept was conceived primarily by S. R., with inputs from A. K. The experiments were designed by A. K., S. D., and S. R. Most of the experiments were performed by A. K. with the help from S. D. and P. B. SEM was performed by M. S. and ITC by T. M., P. B. and A. K. Manuscript was written by S. R., A. K. and S. D. with comments from other authors.

Conflicts of interest

The authors declare no competing financial interest.

Acknowledgements

S. R. acknowledges major financial support from MoE-STARS (STARS/APR2019/BS/820/FS). The Science and Engineering Research Board (CRG/2022/009021) is acknowledged for financial support to access the IISc central facilities. Seed funding by the IISc Digital Health Initiative is acknowledged for part

consumables. The authors are thankful to the Department of Science and Technology (DST-FIST: SR/FST/PSII009/2010) for the instrumental facility at MRC. A. K. and P. B. are thankful to Prime Minister Research Fellowship for doctoral research. M. S. and T. M. are thankful to UGC and MoE, respectively, for the doctoral research fellowships. Financial support from the DBT-RA Program in Biotechnology and Life Sciences is gratefully acknowledged by S. D.

References

1 M. Mofatteh, F. Echegaray-Iturra, A. Alamban, F. Dalla Ricca, A. Bakshi and M. G. Aydogan, Autonomous clocks that regulate organelle biogenesis, cytoskeletal organization, and intracellular dynamics, *eLife*, 2021, **10**, e72104.
2 R. P. Bhattacharyya, A. Reményi, B. J. Yeh and W. A. Lim, Domains, motifs, and scaffolds: the role of modular interactions in the evolution and wiring of cell signaling circuits, *Annu. Rev. Biochem.*, 2006, **75**(1), 655–680.
3 B. N. Kholodenko, J. F. Hancock and W. Kolch, Signalling ballet in space and time, *Nat. Rev. Mol. Cell Biol.*, 2010, **11**(6), 414–426.
4 S. P. W. Wijnands, W. Engelen, R. P. M. Lafleur, E. W. Meijer and M. Merkx, Controlling protein activity by dynamic recruitment on a supramolecular polymer platform, *Nat. Commun.*, 2018, **9**(1), 65.
5 H. Seo and H. Lee, Spatiotemporal control of signal-driven enzymatic reaction in artificial cell-like polymersomes, *Nat. Commun.*, 2022, **13**(1), 5179.
6 S. Zhu, L. Nih, S. T. Carmichael, Y. Lu and T. Segura, Enzyme-Responsive Delivery of Multiple Proteins with Spatiotemporal Control, *Adv. Mater.*, 2015, **27**(24), 3620–3625.
7 A. H. Chen and P. A. Silver, Designing biological compartmentalization, *Trends Cell Biol.*, 2012, **22**(12), 662–670.
8 M. C. Good, J. G. Zalatan and W. A. Lim, Scaffold proteins: hubs for controlling the flow of cellular information, *Science*, 2011, **332**(6030), 680–686.
9 J. Boekhoven, W. E. Hendriksen, G. J. Koper, R. Eelkema and J. H. van Esch, Transient assembly of active materials fueled by a chemical reaction, *Science*, 2015, **349**(6252), 1075–1079.
10 T. A. Ngo, E. Nakata, M. Saimura and T. Morii, Spatially Organized Enzymes Drive Cofactor-Coupled Cascade Reactions, *J. Am. Chem. Soc.*, 2016, **138**(9), 3012–3021.
11 L. Xin, C. Zhou, Z. Yang and D. Liu, Regulation of an Enzyme Cascade Reaction by a DNA Machine, *Small*, 2013, **9**(18), 3088–3091.
12 D. A. Fletcher and R. D. Mullins, Cell mechanics and the cytoskeleton, *Nature*, 2010, **463**(7280), 485–492.
13 S. F. Banani, H. O. Lee, A. A. Hyman and M. K. Rosen, Biomolecular condensates: organizers of cellular biochemistry, *Nat. Rev. Mol. Cell Biol.*, 2017, **18**(5), 285–298.
14 Y. Shin and C. P. Brangwynne, Liquid phase condensation in cell physiology and disease, *Science*, 2017, **357**(6357), eaaf4382.
15 J. B. Casaletto and A. I. McClatchey, Spatial regulation of receptor tyrosine kinases in development and cancer, *Nat. Rev. Cancer*, 2012, **12**(6), 387–400.
16 N. C. Hartman and J. T. Groves, Signaling clusters in the cell membrane, *Curr. Opin. Cell Biol.*, 2011, **23**(4), 370–376.
17 S. M. Albelda and C. A. Buck, Integrins and other cell adhesion molecules, *FASEB J.*, 1990, **4**(11), 2868–2880.
18 M. Mammen, S. K. Choi and G. M. Whitesides, Polyvalent interactions in biological systems: implications for design and use of multivalent ligands and inhibitors, *Angew. Chem., Int. Ed.*, 1998, **37**(20), 2754–2794.
19 K. Nasmyth and C. H. Haering, Cohesin: its roles and mechanisms, *Annu. Rev. Genet.*, 2009, **43**, 525–558.
20 S. L. Schreiber, The Rise of Molecular Glues, *Cell*, 2021, **184**(1), 3–9.
21 K. Okuro, K. Kinbara, K. Takeda, Y. Inoue, A. Ishijima and T. Aida, Adhesion Effects of a Guanidinium Ion Appended Dendritic "Molecular Glue" on the ATP-Driven Sliding Motion of Actomyosin, *Angew. Chem., Int. Ed.*, 2010, **49**(17), 3030–3033.
22 F. Li, I. A. M. Aljahdali and X. Ling, Molecular Glues: Capable Protein-Binding Small Molecules That Can Change Protein–Protein Interactions and Interactomes for the Potential Treatment of Human Cancer and Neurodegenerative Diseases, *Int. J. Mol. Sci.*, 2022, **23**(11), 6206.
23 R. Mogaki, K. Okuro, R. Ueki, S. Sando and T. Aida, Molecular Glue that Spatiotemporally Turns on Protein–Protein Interactions, *J. Am. Chem. Soc.*, 2019, **141**(20), 8035–8040.
24 R. Mogaki, K. Okuro and T. Aida, Molecular glues for manipulating enzymes: trypsin inhibition by benzamidine-conjugated molecular glues, *Chem. Sci.*, 2015, **6**(5), 2802–2805.
25 K. Okuro, M. Sasaki and T. Aida, Boronic Acid-Appended Molecular Glues for ATP-Responsive Activity Modulation of Enzymes, *J. Am. Chem. Soc.*, 2016, **138**(17), 5527–5530.
26 D. St-Cyr, D. F. Ceccarelli, S. Orlicky, A. M. van der Sloot, X. Tang, S. Kelso, S. Moore, C. James, G. Posternak, J. Coulombe-Huntington, T. Bertomeu, A. Marinier, F. Sicheri and M. Tyers, Identification and optimization of molecular glue compounds that inhibit a noncovalent E2 enzyme-ubiquitin complex, *Sci. Adv.*, 2021, **7**(44), eabi5797.
27 J. Vonnemann, C. Sieben, C. Wolff, K. Ludwig, C. Böttcher, A. Herrmann and R. Haag, Virus inhibition induced by polyvalent nanoparticles of different sizes, *Nanoscale*, 2014, **6**(4), 2353–2360.
28 Y. Ouyang, P. Zhang and I. Willner, Dissipative biocatalytic cascades and gated transient biocatalytic cascades driven by nucleic acid networks, *Sci. Adv.*, 2022, **8**(18), eabn3534.
29 A. Mishra, S. Dhiman and S. J. George, ATP-Driven Synthetic Supramolecular Assemblies: From ATP as a Template to Fuel, *Angew. Chem., Int. Ed.*, 2021, **60**(6), 2740–2756.
30 S. A. P. van Rossum, M. Tena-Solsona, J. H. van Esch, R. Eelkema and J. Boekhoven, Dissipative out-of-equilibrium assembly of man-made supramolecular materials, *Chem. Soc. Rev.*, 2017, **46**(18), 5519–5535.

31 L. Zhou, Y. Fan, Z. Liu, L. Chen, E. Spruijt and Y. Wang, A Multiresponsive Transformation between Surfactant-Based Coacervates and Vesicles, *CCS Chem.*, 2021, **3**(12), 358–366.
32 S. Debnath, S. Roy and R. V. Ulijn, Peptide Nanofibers with Dynamic Instability through Nonequilibrium Biocatalytic Assembly, *J. Am. Chem. Soc.*, 2013, **135**(45), 16789–16792.
33 E. Te Brinke, J. Groen, A. Herrmann, H. A. Heus, G. Rivas, E. Spruijt and W. T. Huck, Dissipative adaptation in driven self-assembly leading to self-dividing fibrils, *Nat. Nanotechnol.*, 2018, **13**(9), 849–855.
34 H. Zhao, S. Sen, T. Udayabhaskararao, M. Sawczyk, K. Kučanda, D. Manna, P. K. Kundu, J.-W. Lee, P. Král and R. Klajn, Reversible trapping and reaction acceleration within dynamically self-assembling nanoflasks, *Nat. Nanotechnol.*, 2016, **11**(1), 82–88.
35 P. K. Kundu, D. Samanta, R. Leizrowice, B. Margulis, H. Zhao, M. Börner, T. Udayabhaskararao, D. Manna and R. Klajn, Light-controlled self-assembly of non-photoresponsive nanoparticles, *Nat. Chem.*, 2015, **7**(8), 646–652.
36 S. Das, T. Das, P. Das and D. Das, Controlling the lifetime of cucurbit[8]uril based self-abolishing nanozymes, *Chem. Sci.*, 2022, **13**(14), 4050–4057.
37 M. Solra, S. Das, A. Srivastava, B. Sen and S. Rana, Temporally Controlled Multienzyme Catalysis Using a Dissipative Supramolecular Nanozyme, *ACS Appl. Mater. Interfaces*, 2022, **14**(40), 45096–45109.
38 S. Das, P. Das, P. Dowari, B. K. Das and D. Das, Bi-directional feedback controlled transience in Cucurbituril based tandem nanozyme, *J. Colloid Interface Sci.*, 2022, **614**, 172–180.
39 A. Mishra, D. B. Korlepara, M. Kumar, A. Jain, N. Jonnalagadda, K. K. Bejagam, S. Balasubramanian and S. J. George, Biomimetic temporal self-assembly via fuel-driven controlled supramolecular polymerization, *Nat. Commun.*, 2018, **9**(1), 1295.
40 M. A. Cardona and L. J. Prins, ATP-fuelled self-assembly to regulate chemical reactivity in the time domain, *Chem. Sci.*, 2020, **11**(6), 1518–1522.
41 M. Abbas, W. P. Lipiński, K. K. Nakashima, W. T. S. Huck and E. Spruijt, A short peptide synthon for liquid–liquid phase separation, *Nat. Chem.*, 2021, **13**(11), 1046–1054.
42 P. S. Schwarz, L. Tebcharani, J. E. Heger, P. Müller-Buschbaum and J. Boekhoven, Chemically fueled materials with a self-immolative mechanism: transient materials with a fast on/off response, *Chem. Sci.*, 2021, **12**(29), 9969–9976.
43 T. Heuser, E. Weyandt and A. Walther, Biocatalytic Feedback-Driven Temporal Programming of Self-Regulating Peptide Hydrogels, *Angew. Chem., Int. Ed.*, 2015, **54**(45), 13258–13262.
44 S. Maiti, I. Fortunati, C. Ferrante, P. Scrimin and L. J. Prins, Dissipative self-assembly of vesicular nanoreactors, *Nat. Chem.*, 2016, **8**(7), 725–731.
45 M. R. Wilson, J. Solà, A. Carlone, S. M. Goldup, N. Lebrasseur and D. A. Leigh, An autonomous chemically fuelled small-molecule motor, *Nature*, 2016, **534**(7606), 235–240.
46 R. Rikken, H. Engelkamp, R. Nolte, J. Maan, J. Van Hest, D. Wilson and P. Christianen, Shaping polymersomes into predictable morphologies via out-of-equilibrium self-assembly, *Nat. Commun.*, 2016, **7**(1), 1–7.
47 O. Rifaie-Graham, J. Yeow, A. Najer, R. Wang, R. Sun, K. Zhou, T. N. Dell, C. Adrianus, C. Thanapongpibul, M. Chami, S. Mann, J. R. de Alaniz and M. M. Stevens, Photoswitchable gating of non-equilibrium enzymatic feedback in chemically communicating polymersome nanoreactors, *Nat. Chem.*, 2023, **15**, 110–118.
48 A. Sorrenti, J. Leira-Iglesias, A. Sato and T. M. Hermans, Non-equilibrium steady states in supramolecular polymerization, *Nat. Commun.*, 2017, **8**(1), 1–8.
49 G. Liu, J. Tan, J. Cen, G. Zhang, J. Hu and S. Liu, Oscillating the local milieu of polymersome interiors via single input-regulated bilayer crosslinking and permeability tuning, *Nat. Commun.*, 2022, **13**(1), 585.
50 A. Belluati, S. Thamboo, A. Najer, V. Maffeis, C. von Planta, I. Craciun, C. G. Palivan and W. Meier, Multicompartment Polymer Vesicles with Artificial Organelles for Signal-Triggered Cascade Reactions Including Cytoskeleton Formation, *Adv. Funct. Mater.*, 2020, **30**(32), 2002949.
51 V. Maffeis, A. Belluati, I. Craciun, D. Wu, S. Novak, C.-A. Schoenenberger and C. G. Palivan, Clustering of catalytic nanocompartments for enhancing an extracellular non-native cascade reaction, *Chem. Sci.*, 2021, **12**(37), 12274–12285.
52 L. Schoonen and J. C. M. van Hest, Compartmentalization Approaches in Soft Matter Science: From Nanoreactor Development to Organelle Mimics, *Adv. Mater.*, 2016, **28**(6), 1109–1128.
53 X. Hao, K. Yang, H. Wang, F. Peng and H. Yang, Biocatalytic feedback-controlled non-Newtonian fluids, *Angew. Chem., Int. Ed.*, 2020, **59**(11), 4314–4319.
54 H. Che, B. C. Buddingh' and J. C. van Hest, Self-Regulated and Temporal Control of a "Breathing" Microgel Mediated by Enzymatic Reaction, *Angew. Chem.*, 2017, **129**(41), 12755–12759.
55 F. Schnitter, A. M. Bergmann, B. Winkeljann, J. Rodon Fores, O. Lieleg and J. Boekhoven, Synthesis and characterization of chemically fueled supramolecular materials driven by carbodiimide-based fuels, *Nat. Protoc.*, 2021, **16**(8), 3901–3932.
56 M. G. Howlett, A. H. J. Engwerda, R. J. H. Scanes and S. P. Fletcher, An autonomously oscillating supramolecular self-replicator, *Nat. Chem.*, 2022, **14**(7), 805–810.
57 E. Del Grosso, G. Ragazzon, L. J. Prins and F. Ricci, Fuel-responsive allosteric DNA-based aptamers for the transient release of ATP and cocaine, *Angew. Chem.*, 2019, **131**(17), 5638–5642.
58 J. Wang, Z. Li and I. Willner, Cascaded dissipative DNAzyme-driven layered networks guide transient replication of coded-strands as gene models, *Nat. Commun.*, 2022, **13**(1), 4414.
59 D. B. Craig and C. J. Wallace, ATP binding to cytochrome c diminishes electron flow in the mitochondrial respiratory pathway, *Protein Sci.*, 1993, **2**(6), 966–976.

60 D. B. McIntosh, J. C. Parrish and C. J. Wallace, Definition of a nucleotide binding site on cytochrome c by photoaffinity labeling, *J. Biol. Chem.*, 1996, **271**(31), 18379–18386.
61 A. Narunsky, A. Kessel, R. Solan, V. Alva, R. Kolodny and N. Ben-Tal, On the evolution of protein-adenine binding, *Proc. Natl. Acad. Sci. U. S. A.*, 2020, **117**(9), 4701–4709.
62 P. Chakrabarti and U. Samanta, CH/pi interaction in the packing of the adenine ring in protein structures, *J. Mol. Biol.*, 1995, **251**(1), 9–14.
63 M. Onda, K. Yoshihara, H. Koyano, K. Ariga and T. Kunitake, Molecular Recognition of Nucleotides by the Guanidinium Unit at the Surface of Aqueous Micelles and Bilayers. A Comparison of Microscopic and Macroscopic Interfaces, *J. Am. Chem. Soc.*, 1996, **118**(36), 8524–8530.
64 S. Dey, T. Sarkar, A. Majumdar, T. Pathak and K. Ghosh, 1,4-Disubstituted 1,2,3-Triazole- and 1,5-Disubstituted 1,2,3-Triazole-based Bis-Sulfonamides in Selective Fluorescence Sensing of ATP, *ChemistrySelect*, 2017, **2**(6), 2034–2038.
65 N. Comfort, K. Cai, T. R. Bloomquist, M. D. Strait, A. W. Ferrante Jr and A. A. Baccarelli, Nanoparticle Tracking Analysis for the Quantification and Size Determination of Extracellular Vesicles, *J. Visualized Exp.*, 2021, **169**, e62447.
66 M. Abbas, J. O. Law, S. N. Grellscheid, W. T. S. Huck and E. Spruijt, Peptide-Based Coacervate-Core Vesicles with Semipermeable Membranes, *Adv. Mater.*, 2022, **34**(34), 2202913.
67 A. Wang, C. C. Miller and J. Szostak, Interpreting turbidity measurements for vesicle studies, *bioRxiv*, 2018, preprint, bioRxiv:348904, DOI: **10.1101/348904**.
68 H. Fan, K. Li, T. Tu, X. Zhu, L. Zhang and M. Liu, ATP-Induced Emergent Circularly Polarized Luminescence and Encryption, *Angew. Chem., Int. Ed.*, 2022, **61**(19), e202200727.
69 M. S. Ganewatta, Y. P. Chen, J. Wang, J. Zhou, J. Ebalunode, M. Nagarkatti, A. W. Decho and C. Tang, Bio-inspired resin acid-derived materials as anti-bacterial resistance agents with unexpected activities, *Chem. Sci.*, 2014, **5**(5), 2011–2016.
70 Q. Wang, B. Lin, M. Chen, C. Zhao, H. Tian and D.-H. Qu, A dynamic assembly-induced emissive system for advanced information encryption with time-dependent security, *Nat. Commun.*, 2022, **13**(1), 4185.
71 H. Wang, Y. Wang, B. Shen, X. Liu and M. Lee, Substrate-Driven Transient Self-Assembly and Spontaneous Disassembly Directed by Chemical Reaction with Product Release, *J. Am. Chem. Soc.*, 2019, **141**(10), 4182–4185.
72 J. U. De Mel, S. Gupta, R. M. Perera, L. Ngo, P. Zolnierczuk, M. Bleuel, S. V. Pingali and G. J. Schneider, Influence of External NaCl Salt on Membrane Rigidity of Neutral DOPC Vesicles, *Langmuir*, 2020, **36**(32), 9356–9367.
73 A. Schena, R. Griss and K. Johnsson, Modulating protein activity using tethered ligands with mutually exclusive binding sites, *Nat. Commun.*, 2015, **6**(1), 7830.
74 M. Hüttemann, P. Pecina, M. Rainbolt, T. H. Sanderson, V. E. Kagan, L. Samavati, J. W. Doan and I. Lee, The multiple functions of cytochrome c and their regulation in life and death decisions of the mammalian cell: from respiration to apoptosis, *Mitochondrion*, 2011, **11**(3), 369–381.
75 A. Amat, J. Rigau, R. W. Waynant, I. K. Ilev, J. Tomas and J. J. Anders, Modification of the intrinsic fluorescence and the biochemical behavior of ATP after irradiation with visible and near-infrared laser light, *J. Photochem. Photobiol., B*, 2005, **81**(1), 26–32.
76 D. J. Woodbury, E. C. Whitt and R. E. Coffman, A review of TNP-ATP in protein binding studies: benefits and pitfalls, *Biophys. Rep.*, 2021, **1**(1), 100012.
77 C. Corbo, R. Molinaro, F. Taraballi, N. E. Toledano Furman, M. B. Sherman, A. Parodi, F. Salvatore and E. Tasciotti, Effects of the protein corona on liposome-liposome and liposome-cell interactions, *Int. J. Nanomed.*, 2016, **11**, 3049–3063.
78 J. Xu, T. K. Vanderlick and P. A. Beales, Lytic and non-lytic permeabilization of cardiolipin-containing lipid bilayers induced by cytochrome C, *PLoS One*, 2013, **8**(7), e69492.
79 P. Compain, C. Decroocq, J. Iehl, M. Holler, D. Hazelard, T. Mena Barragán, C. Ortiz Mellet and J.-F. Nierengarten, Glycosidase Inhibition with Fullerene Iminosugar Balls: A Dramatic Multivalent Effect, *Angew. Chem., Int. Ed.*, 2010, **49**(33), 5753–5756.
80 C. Bonduelle, J. Huang, T. Mena-Barragán, C. Ortiz Mellet, C. Decroocq, E. Etamé, A. Heise, P. Compain and S. Lecommandoux, Iminosugar-based glycopolypeptides: glycosidase inhibition with bioinspired glycoprotein analogue micellar self-assemblies, *Chem. Commun.*, 2014, **50**(25), 3350–3352.
81 N. Kanfar, E. Bartolami, R. Zelli, A. Marra, J.-Y. Winum, S. Ulrich and P. Dumy, Emerging trends in enzyme inhibition by multivalent nanoconstructs, *Org. Biomol. Chem.*, 2015, **13**(39), 9894–9906.
82 L. Wu and X. Jiang, Enhancing Peroxidase Activity of Cytochrome c by Modulating Interfacial Interaction Forces with Graphene Oxide, *Langmuir*, 2020, **36**(5), 1094–1102.
83 S. Rani, B. Dasgupta, G. K. Bhati, K. Tomar, S. Rakshit and S. Maiti, Superior Proton-Transfer Catalytic Promiscuity of Cytochrome c in Self-Organized Media, *ChemBioChem*, 2021, **22**(7), 1285–1291.
84 B. S. Sandanaraj, H. Bayraktar, K. Krishnamoorthy, M. J. Knapp and S. Thayumanavan, Recognition and Modulation of Cytochrome c's Redox Properties using an Amphiphilic Homopolymer, *Langmuir*, 2007, **23**(7), 3891–3897.
85 A. M. Carver, M. De, H. Bayraktar, S. Rana, V. M. Rotello and M. J. Knapp, Intermolecular electron-transfer catalyzed on nanoparticle surfaces, *J. Am. Chem. Soc.*, 2009, **131**(11), 3798–3799.
86 H. Jia, G. Zhu and P. Wang, Catalytic behaviors of enzymes attached to nanoparticles: the effect of particle mobility, *Biotechnol. Bioeng.*, 2003, **84**(4), 406–414.
87 L. Stefan, F. Denat and D. Monchaud, Insights into how nucleotide supplements enhance the peroxidase-mimicking DNAzyme activity of the G-quadruplex/hemin system, *Nucleic Acids Res.*, 2012, **40**(17), 8759–8772.

88 A. Chatterjee, C. Mahato and D. Das, Complex Cascade Reaction Networks via Cross β Amyloid Nanotubes, *Angew. Chem., Int. Ed.*, 2021, **60**(1), 202–207.

89 L. Li, K. Chen, Y. Wu, G. Xiang and X. Liu, Epigenome–Metabolome–Epigenome signaling cascade in cell biological processes, *J. Genet. Genomics*, 2022, **49**(4), 279–286.

90 I. I. Moraru and L. M. Loew, Intracellular signaling: spatial and temporal control, *Physiology*, 2005, **20**(3), 169–179.

91 D. C. Miller, S. V. Athavale and F. H. Arnold, Combining chemistry and protein engineering for new-to-nature biocatalysis, *Nat. Synth.*, 2022, **1**(1), 18–23.

92 S. M. Assadi, M. Yücel and C. Pantelis, Dopamine modulates neural networks involved in effort-based decision-making, *Neurosci. Biobehav. Rev.*, 2009, **33**(3), 383–393.

93 R. H. Kang, Y. Kim, J. H. Kim, N. H. Kim, H. M. Ko, S.-H. Lee, I. Shim, J. S. Kim, H.-J. Jang and D. Kim, Self-Activating Therapeutic Nanoparticle: A Targeted Tumor Therapy Using Reactive Oxygen Species Self-Generation and Switch-on Drug Release, *ACS Appl. Mater. Interfaces*, 2021, **13**(26), 30359–30372.